

Spring 5-1-2022

Minimal Inscribed Polyforms

Jack Hanke
jack.hanke@uconn.edu

Follow this and additional works at: https://opencommons.uconn.edu/srhonors_theses



Part of the [Mathematics Commons](#)

Recommended Citation

Hanke, Jack, "Minimal Inscribed Polyforms" (2022). *Honors Scholar Theses*. 916.
https://opencommons.uconn.edu/srhonors_theses/916

Minimal Inscribed Polyforms

Jack Hanke

April 2022

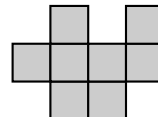
An Undergraduate Honors Thesis
Submitted in Partial Fulfillment of the
Requirements for the Degree of
Bachelor of Arts with Honors
at the
University of Connecticut

1 Introduction

A *polyomino of area n* is a shape in \mathbb{Z}^2 constructed by joining n unit squares along their edges. A domino is the case $n = 2$. Polyominos of area n are often referred to as n -ominos.



A domino (2-omino)



An 8-omino

Polyominos were first given serious mathematical attention by Solomon Golomb in 1953 [Kla67] and were popularized by Martin Gardner in his “Mathematical Games” column in the October 1965 issue of Scientific American [Gar65]. Polyominos, often referred to as “animals” in the physics and chemistry literature, are used in both the Ising Model for magnetism and the modeling of branch polymers [PS81].

A question one might ask is exactly how many n -ominos are there? Similarly, how does the number of n -ominos grow in n ? To examine this question, we must first make our definition of polyomino more precise.

This thesis will first examine the formal definition of a polyomino and the common equivalence classes polyominos are enumerated under. We then turn to polyomino families, and provide exact enumeration results for certain families, including the minimal inscribed polyominos. Next we will generalize polyominos to polyforms, and provide novel formulae for polyform analogues of minimal inscribed polyominos. Finally, we discuss some further questions concerning minimal inscribed polyforms.

2 Definitions

In this section we introduce common terminology used in the study of polyominos. We begin by precisely defining what a polyomino is, followed by a discussion of holes. After that, common equivalence classes are defined leading to different enumeration problems.

2.1 What is a polyomino?

Polyominos were first introduced as a generalization of dominos. Informally, a *polyomino of area n* is a figure in the plane constructed by joining n unit squares, called *cells*, edge to edge. This paper will also use a more formal definition, which we build up in terms of graph theory.

Definition 2.1. A *simple graph* $G = (V, E)$ on n vertices consists of a *vertex set* $V = \{v_1, \dots, v_n\}$ and an *edge set* $E \subseteq \{\{v, w\} | v, w \in V \text{ and } v \neq w\}$.

A simple graph can also be thought of as a diagram, where V is the set of vertices and E is the set of segments drawn between them.

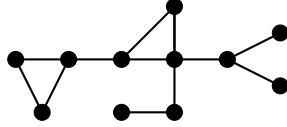


Figure 1: A simple graph G with 11 vertices and 12 edges

From here on, all uses of the term “graph” will mean “simple graph.”

Definition 2.2. In a graph $G = (V, E)$, a *path* between v_1 and v_{k+1} of length k is a set of distinct vertices $v_1, \dots, v_{k+1} \subset V$ and a corresponding set of distinct edges $e_1, \dots, e_k \subset E$ such that $e_i = \{v_i, v_{i+1}\}, \forall i \in \{1, \dots, k\}$.

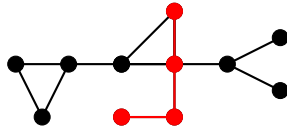


Figure 2: A path of length 3 in G

Paths are used to define how a graph is *connected*. In Figure 2 the path is shown in red.

Definition 2.3. A graph $G = (V, E)$ is *connected* if for any two vertices $v, w \in V$, there exists a path P between v and w .



A connected graph



A graph that is not connected

Finally, we can define *subgraphs* as graphs within graphs.

Definition 2.4. A *subgraph* $H = (V', E')$ of $G = (V, E)$ is a graph with vertex set $V' \subset V$ and $E' \subset E$.

The highlighted path in Figure 2 also serves as a subgraph in G . Now that we have defined graphs, which graph is needed to construct polyominoes?

If we consider the elements $(n, m) \in \mathbb{Z}^2$ as vertices on the plane, and join all points (n_1, m_1) and (n_2, m_2) that have $|n_1 - n_2| + |m_1 - m_2| = 1$ by a segment, we arrive at the *square lattice* graph.

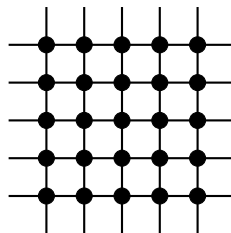


Figure 3: The square lattice

The square lattice is where we will construct polyominoes. By taking connected subgraphs of the square lattice, one can make shapes that represent polyominoes.

There is a problem with this. By convention, a polyomino is considered the same regardless of its location. However, one can find many subgraphs that look the same in the square lattice, except in different locations. To fix this, the formal definition asserts that all subgraphs that can be shifted to a different location, but otherwise retain their shape, are the same polyomino. This shifting of location while maintaining shape is called *translation*. When an object is considered the same regardless of the location it is found in, it is said to be the “same up to translation”. Finally, we reach the formal definition.

Definition 2.5. A *polyomino* is a finite connected subgraph of the square lattice, up to translation.

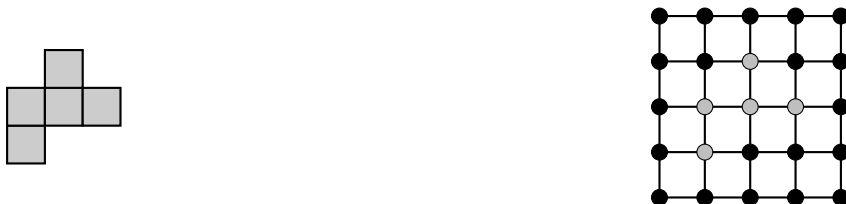
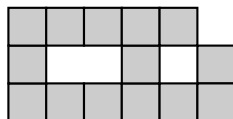


Figure 4: A polyomino and a corresponding subgraph of the square lattice

Definition 2.5 is often called the **dual graph** definition of polyominoes. It will be beneficial to keep both the informal and dual graph definitions in mind. Definition 2.5 will be especially useful for the main results of the paper in Section 4. By convention, however, the term “cells” will often replace “vertices.”

2.2 Holes

Notice that our definitions allow for finite connected components that are not part of the polyomino to be completely surrounded by the polyomino. These components are called *holes*.



A polyomino with two holes

Some older polyomino literature disallows holes. The class of polyominoes that does not contain holes is called “polygons”. The enumeration of polygons is also interesting, but won’t be studied here.

Surprisingly, there are strong results for the number of holes in a polyomino of size n . Kahle and Roldán [KR18] give bounds for the maximal number of holes that a polyomino of area n can enclose and construct polyominoes that are known to have the maximal number of holes for certain n .

Definition 2.5 is useful in identifying whether or not a subgraph of the square lattice is a polyomino or not. However, polyominoes can still look similar to one another. What does one consider as a different polyomino?

2.3 Equivalence Classes

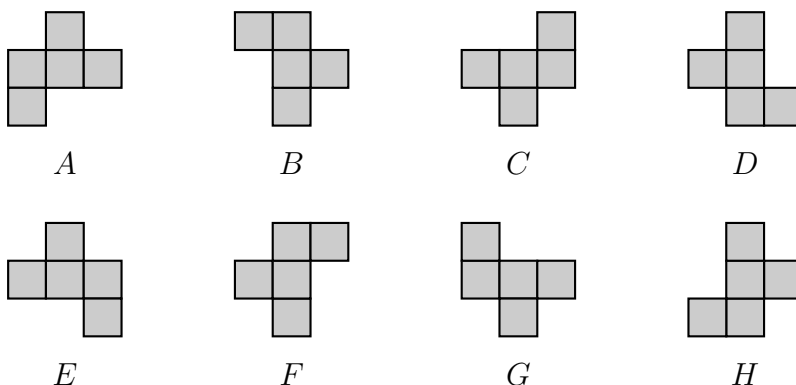
Classically, there are three main classes of polyominoes: fixed, chiral, and free. These classes are distinguished by which types of symmetries constitute the same polyomino.

Definition 2.6. The class of *fixed* polyominoes of area n consists of all connected subgraphs of the square lattice up to translation, regardless of other symmetries.

Definition 2.7. The class of *chiral* polyominoes of area n are the fixed polyominoes that are rotationally distinct.

Definition 2.8. The class of *free* polyominoes of area n are the fixed polyominoes that are distinct under rotations and reflections.

An example of each equivalence class can be seen with the following set of 8 fixed polyominoes.



This set contains 2 different chiral polyominoes. Polyominoes B , C , and D can all be reached by rotating polyomino A clockwise. Similarly, polyominoes F , G , and H can all be reached by rotating polyomino E counter-clockwise. However, no polyominoes in the top row can be reached by rotating any polyominoes in the bottom row. So we have two rotationally distinct sets, and consequently 2 different chiral polyominoes.

The above set contains a single free polyomino. Polyomino E can be reached by reflecting polyomino A across the y -axis. Rotating A and E reaches the remaining polyominoes. Therefore, each of these polyominoes are rotations or reflections of each other, and so only represent 1 free polyomino.



The single free domino



The two free 3-ominoes

A popular example of equivalence classes is the TETRIS pieces, consisting of all of the chiral 4-ominoes. Figure 5 shows all 19 fixed 4-ominoes. However, in TETRIS the pieces are considered the same regardless of how they are rotated and so are colored by the chiral equivalence class.

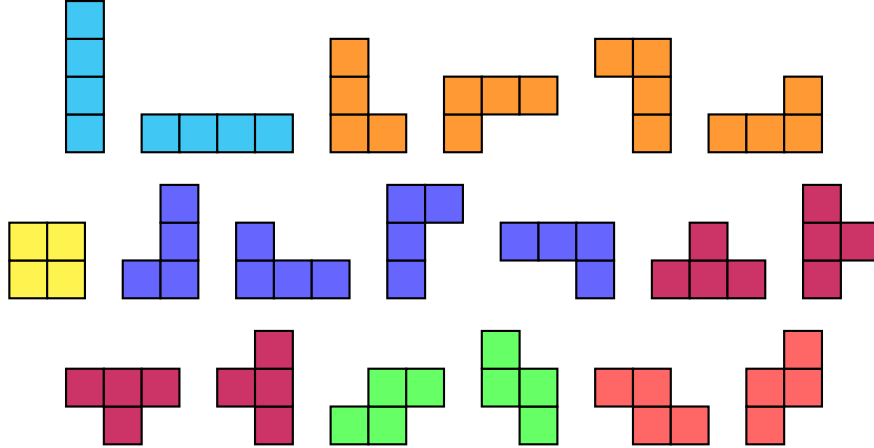


Figure 5: All fixed 4-ominoes, colored by the different chiral 4-ominoes

Suppose we call the number of fixed n -ominoes t_n , the number of chiral n -ominoes r_n , and the number of free n -ominoes s_n . It follows that

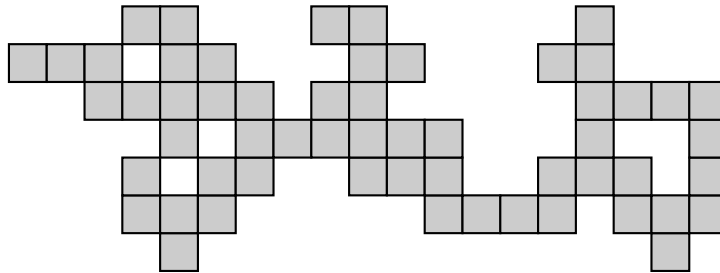
$$\frac{t_n}{8} \leq s_n \leq r_n \leq t_n \quad (1)$$

from the dihedral symmetries of the square lattice.

The first few terms of the number of s_n , r_n , and t_n for $n \geq 1$, are summarized in the table below.

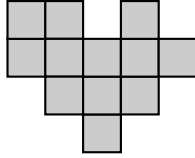
n	1	2	3	4	5	6	7	8	9	10
t_n	1	2	6	19	63	216	760	2725	9910	36446
r_n	1	1	2	7	18	60	196	704	2500	9189
s_n	1	1	2	5	12	35	108	369	1285	4655

The reader can verify that $t_4 = 19$ and $r_4 = 7$ from Figure 5. They can also verify that $s_4 = 5$, as the orange and blue polyominoes are the same free polyomino, as well as the green and red polyominoes. Both free and fixed polyominoes have been enumerated up to $n = 56$ by Jensen [Jen01].

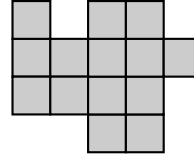


A 56-omino

Given the simplicity of their definition, it is surprising that there is no closed formula known for the number of fixed, chiral, or free polyominoes of a given area n . Although an exact formula remains elusive, it is known that the sequence is exponential in n . The table below shows the first couple of values of $(t_n)^{\frac{1}{n}}$ and $\frac{t_{n+1}}{t_n}$.



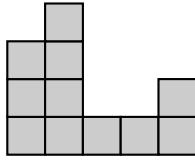
A column-convex 10-omino



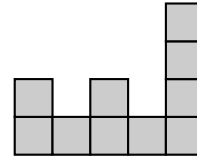
A column-convex 14-omino

Row-convex polyominoes are defined similarly. The following family will be the first family that we can exactly enumerate.

Definition 3.3. A polyomino is a *bargraph* if it is north-east and north-west directed, and column convex.



A bargraph 11-omino

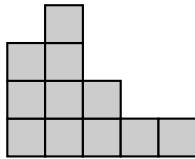


A bargraph 10-omino

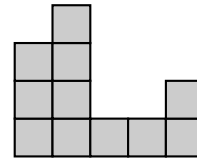
Enumerating the number b_n , of bargraph polyominoes with area n under the fixed equivalence class is straightforward.

Proposition 1. *The number of bargraph n -ominoes $b_n = 2^{n-1}$.*

Proof. Suppose we have a bargraph polyomino of area n . Notice that for $n \geq 2$, bargraph polyominoes are of two types: those that have right-most column of height 1, and those that have height 2 or more.

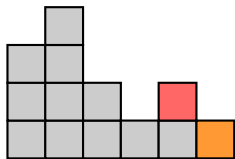


A bargraph of the first type

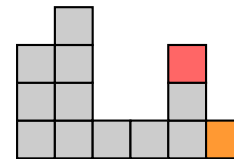


A bargraph of the second type

Next, we will concatenate a unit square in one of two possible places.



Concatenations on bargraphs of the first type



Concatenations on bargraphs of the second type

These concatenations take a bargraph n -omino of a certain type and creates a bargraph $(n+1)$ -omino of each type. The red concatenation makes a bargraph with right-most column height of 2 or more, and the orange concatenation makes a bargraph with right-most column height 1. Because this can be done to any bargraph n -omino, and every bargraph polyomino is created in this way exactly once, this gives $b_{n+1} = 2b_n$. With the base case $b_1 = 1$, we get $b_n = 2^{n-1}$. \square

This is a simple version of a concatenation argument, which appear commonly for exactly-enumerated families. The proof of Proposition 1 also holds under the chiral equivalence class. However, the proof does not hold under the free equivalence class, because we can no longer guarantee that a concatenation creates a unique polyomino. For example, the 8-ominos constructed from the following orange concatenations below would be counted separately but create the same free bargraph polyomino.



Next let us examine a more complicated concatenation argument: the enumeration of north-east directed polyominoes.

Theorem 1 ([Dha82]). *The generating function $D(x)$ for the number of directed n -ominos d_n is*

$$D(x) = \sum_{n \geq 0} d_n x^n = \frac{1}{2} \left(\sqrt{\frac{1+x}{1-3x}} - 1 \right).$$

The proof of Theorem 1 is more involved than that of bargraph polyominoes. We present the proof to show that a simply defined family can often be difficult to exactly count. We follow the proof in [Gut09].

Proof. A directed polyomino can be thought of as a stack of horizontal dimers on a pegboard, where the vertices of the dimers slide down the pegs and rest on the dimers below it. A *dimer* is a graph with two vertices, connected by an edge.



Figure 6: A dimer

If we replace each cell with a dimer, we get a model for directed polyominoes. An example of this is shown in Figure 7. Notice that the source for the directed polyomino is at the bottom of the diagram as opposed to the bottom left.

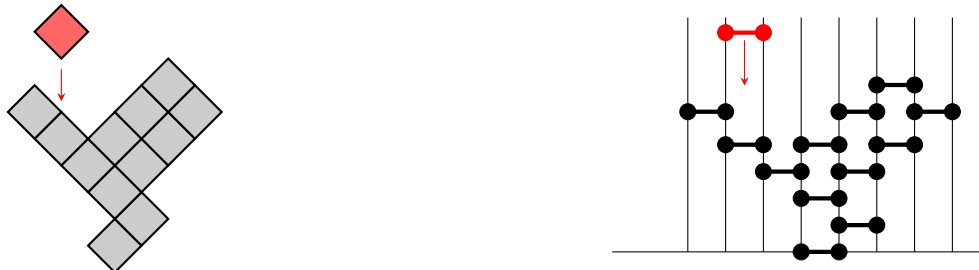


Figure 7: A directed 12-omino with a new red cell being added, and a corresponding dimer representation

We call these stacks of dimers *pyramids*. If a pyramid had no dimers to the column to the left of the source column, we call the pyramid a *half-pyramid*.

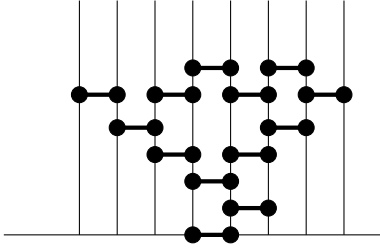


Figure 8: A pyramid

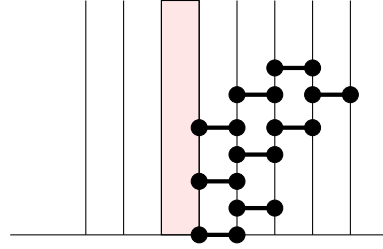


Figure 9: A half-pyramid

In Figure 9, the column to the left of the source column is highlighted in pink. Let us assign h_n to be the number of half-pyramids of area n , and $H(x) = \sum_{n \geq 0} h_n x^n$.

The *product* of two pyramids is defined as putting a pyramid above the other and dropping its pieces. In Figure 10 the source of the above pyramid is labelled in white.

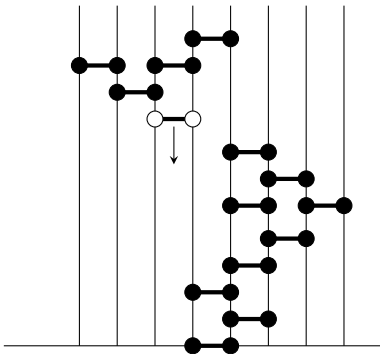


Figure 10: Two pyramids

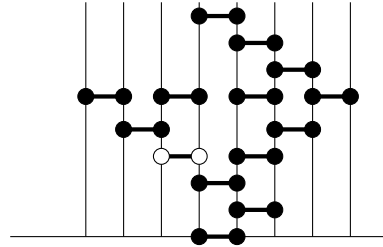


Figure 11: The product of the two pyramids in Figure 10

The key realization is that a pyramid is either a half-pyramid, or the product of a half-pyramid and a pyramid. Visually, if pyramids and half-pyramids are represented by the general diagram shown below

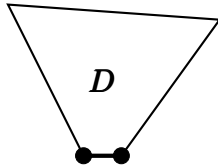


Figure 12: A diagram of a pyramid

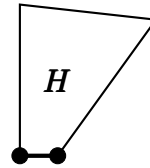
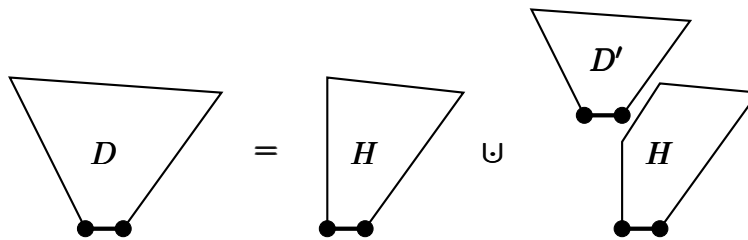


Figure 13: A diagram of a half-pyramid

then we can realize any pyramid as follows



This decomposition corresponds with the following generating function equation

$$D(x) = H(x) + H(x)D(x). \quad (2)$$

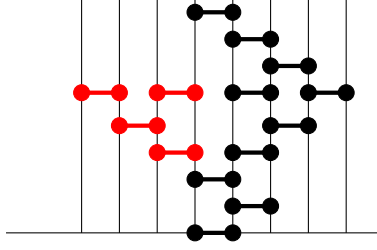
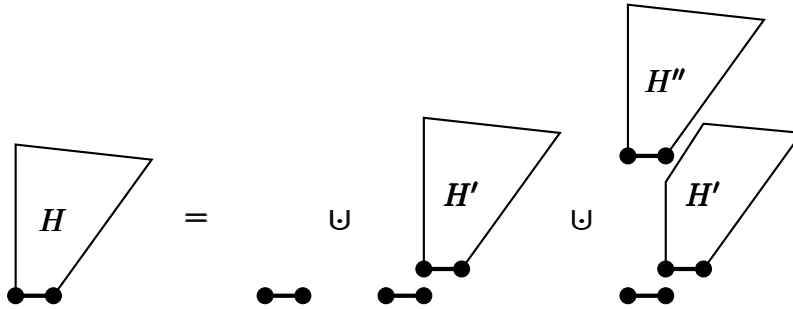


Figure 14: An example of a pyramid being decomposed into a pyramid (red) and a half-pyramid (black)

Half-pyramids can also be decomposed. They can either be just the single source dimer, or the product of a single dimer and a half-pyramid, or the product of a single dimer and two half-pyramids. Visually, the decomposition is



and corresponds with the following generating function equation

$$H(x) = x + xH(x) + xH^2(x). \quad (3)$$

Using the fact that $h_0 = H(0) = 0$, this gives us that $H(x) = \frac{1-x}{2x} - \frac{1}{2x} \sqrt{(1-3x)(1+x)}$. Combining this with $D(x) = \frac{H(x)}{1-H(x)}$, we get that $D(x) = \frac{1}{2} \left(\sqrt{\frac{1+x}{1-3x}} - 1 \right)$. □

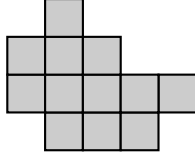
The enumeration of column-convex polyominoes is even more involved.

Theorem 2. *The generating function $C(x)$ for the number of column-convex n -ominoes c_n is*

$$C(x) = \sum_{n \geq 0} c_n x^n = \frac{x(1-x)^3}{1-5x+7x^2-4x^3}.$$

The proof of Theorem 2 can be found in [Tem56]. Regardless of the difficulty in enumeration, column-convex polyominoes have a rational generating function. In contrast, a seemingly natural extension of column-convex polyominoes, the *convex polyominoes*, has no known exact formula or simple generating function.

Definition 3.4. A polyomino is *convex* if it is both column-convex and row-convex.



A convex polyomino

Theorem 3 ([KR74; Ben74]). *The number of convex polyominoes $a_n \sim c\gamma^n$, where $\gamma = 2.30914\dots$ and $c = 2.67564\dots$*

Theorem 3 illustrates that many simply defined families remain without exact formulae.

The main results of this paper are based on the following family of polyominoes.

3.2 Minimal Inscribed Polyominoes

A polyomino family that has been exactly enumerated is the minimal inscribed polyominoes.

Definition 3.5. A polyomino is *minimal inscribed* when it is contained in a $w \times \ell$ rectangular grid, where each of the four sides of the rectangle is touched by a cell of the polyomino, and the polyomino is of minimal area $w + \ell - 1$.

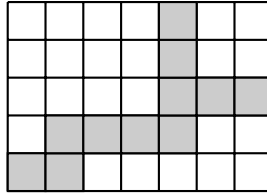


Figure 15: A Minimal Inscribed 11-omino in a 7×5 grid

How many of these polyominoes are there?

Theorem 4 ([GCN10]). *Let $s_{w,\ell}$ be the number of minimal inscribed polyominoes in a given $w \times \ell$ grid. Then $s_{w,\ell} = 8\binom{w+\ell-2}{w-1} - 3w\ell + 2w + 2\ell - 8$.*

So minimally inscribed polyominoes can be counted exactly. In terms of growth rate, setting $\ell = w$ gives a growth rate of 4, as $\binom{2n}{n} \sim \frac{4^n}{\sqrt{\pi n}}$.

We give a new proof of Theorem 4 which is simpler than the original one. First, fix w and ℓ , and call S the set of all $(w + \ell - 1)$ -ominoes that can be inscribed in an $w \times \ell$ grid. S can be split into three subsets based on the number of corners of the rectangle a polyomino touches. S_2 contains polyominoes that contain either 2 or 3 corners, S_1 contains polyominoes that contain 1 corner, and S_0 contains polyominoes that contain no corners. An example of each subset for the 4×4 grid is shown in Figure 16.

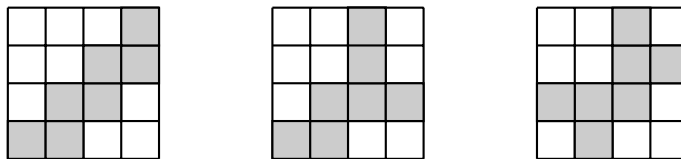


Figure 16: Examples of elements in S_2 , S_1 , and S_0 for a 4×4 grid

What about S_4 , the set of polyominoes that touch all four corners of the rectangular grid?

Proposition 2. *The set S_4 of minimal inscribed polyominoes that touch four corners is empty.*

Proof. Suppose S_4 is nonempty. Consider removing a corner cell v_0 from a polyomino $A \in S_4$. There are two cases. The first case is that the remaining shape is a polyomino A' that touches three corners. This shape is 1 cell smaller than A . However, A' still touches all sides, as it touches three corners of the grid. So A could not have been minimal, and therefore was not in S_4 .

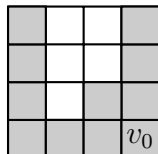


Figure 17: Case 1: Removing v_0 leaves a polyomino

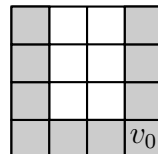


Figure 18: Case 2: Removing v_0 disconnects the polyomino

The second case is that the remaining shape is not a polyomino, and is instead disconnected. As removing a corner cell is removing a cell with at most two adjacent neighboring cells, this disconnection will have split A into a polyomino that touches one corner and a polyomino that touches two corners. Simply deleting all cells from the region that touches one corner, and then returning the original corner cell v_0 leaves a polyomino A' that has area less than A but still has three corners, again contradicting that A was minimal, and consequently that A was in S_4 . Therefore S_4 must be empty. \square

From Proposition 2 we can write

$$S = S_2 \cup S_1 \cup S_0,$$

where S_2 , S_1 , and S_0 are disjoint. We will enumerate S_2 , S_1 , and S_0 to enumerate S . The proof of Theorem 4 is as follows.

Proof. We first split S_2 into two subsets, $S_{T,2}$ and $S_{T,2}^c$ so that $S_{T,2} \cup S_{T,2}^c = S_2$. Let $S_{T,2}$ will represent all polyominoes that are “T-shaped”, while $S_{T,2}^c$ will represent all polyominoes that are not. Formally, the “T-shaped” polyominoes are all polyominoes that contain two adjacent corner cells and a perpendicular bar, as in the left polyomino in Figure 19.

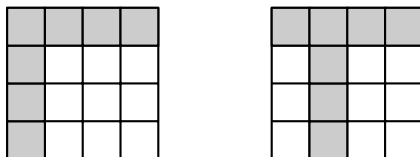


Figure 19: Examples of elements in $S_{T,2}^c$, and $S_{T,2}$ for a 4×4 grid

For $|S_{T,2}|$, it is easy to see that $|S_{T,2}| = 2(w - 2) + 2(\ell - 2) = 2w + 2\ell - 8$.

For $|S_{T,2}^c|$, suppose that the bottom left cell of the $w \times \ell$ grid is called $(1, 1)$, and the top right cell (w, ℓ) . The number of paths from $(1, 1)$ to (w, ℓ) is the number of ways one can make $w - 1$ unit steps right and $\ell - 1$ unit steps up among $w + \ell - 2$ total unit

steps. This gives a total of $\binom{w+\ell-2}{w-1}$ paths from $(1,1)$ to (w,ℓ) . As we can make the same argument for corners $(1,\ell)$ and $(w,1)$, we can conclude $|S_{T,2}^c| = 2\binom{w+\ell-2}{w-1}$. This gives us $|S_2| = |S_{T,2}| + |S_{T,2}^c| = 2\binom{w+\ell-2}{w-1} + 2w + 2\ell - 8$.

Now, consider S_1 . Suppose we choose corner $(1,1)$, and start a path to some point (i,j) . Extending a path from (i,j) to (i,ℓ) and from (i,j) to (w,j) creates a minimally inscribed polyomino that touches only one corner. Notice that (i,j) must have $i \in [2, w-1]$, and $j \in [2, \ell-1]$, as extending the path with i or j outside these ranges would create a polyomino with either two or three corners. Therefore, the total number of polyominoes that touch only corner $(1,1)$ in S_1 is

$$\sum_{i=2}^{w-1} \sum_{j=2}^{\ell-1} \binom{i+j-2}{i-1} = \binom{w+\ell-2}{w-1} - (w+\ell-2)$$

As we can make the same argument starting at any other corner, we have $|S_1| = 4\binom{w+\ell-2}{w-1} - 4w - 4\ell + 8$

Finally, consider S_0 . Suppose we have two points (i,j) and (i',j') , with $i, i' \in [2, w-1]$ and $j, j' \in [2, \ell-1]$. Also initially assume that $i \leq i'$ and $j \leq j'$. One can construct a path from (i,j) to (i',j') . Next, make a path from (i,j) to $(1,j)$, and a path from (i,j) to $(i,1)$. Similarly, make a path from (i',j') to (w,j') and a path from (i',j') to (i',ℓ) . This constructs a polyomino that touches no corners.

These polyominoes can easily be enumerated by the size of the rectangle made with corners (i,j) , (i,j') , (i',j) , and (i',j') . If we suppose that $\Delta i = i' - i$, and $\Delta j = j' - j$, we can construct the following sum.

$$\sum_{\Delta i=1}^{w-2} \sum_{\Delta j=1}^{\ell-2} \binom{\Delta i + \Delta j - 2}{\Delta i - 1} (\ell - 1 - \Delta j)(w - 1 - \Delta i) = \binom{w+\ell-2}{w-1} - w\ell + w + \ell - 2$$

As (i,j') and (i',j) define the same rectangle but different polyominoes, we can multiply the above result by two. However, this double counts the polyominoes that are built with $i = i'$ and $j = j'$. As there are $(w-2)(\ell-2)$ of these polyominoes, we subtract this quantity once. Therefore get that $|S_0| = 2\binom{w+\ell-2}{w-1} - 2w\ell + 2w + 2\ell - 4 - (w-2)(\ell-2) = 2\binom{w+\ell-2}{w-1} - 3w\ell + 4w + 4\ell - 8$

Combining the three subsets, we get the result.

$$|S| = |S_2| + |S_1| + |S_0| = 8\binom{w+\ell-2}{w-1} - 3w\ell + 2w + 2\ell - 8$$

□

4 Extensions to Polyforms

Next we seek to generalize the results from Theorem 4. How can the idea of a polyomino be extended? What can we generalize, and what enumeration questions can we solve?

4.1 Polyforms

What if we append unit triangles along their sides instead of unit squares? Or append unit hexagons? This is the idea behind *polyforms*.

Definition 4.1. A *polyform* of area n is a shape in the plane constructed by joining n unit side length polygons along their edges.

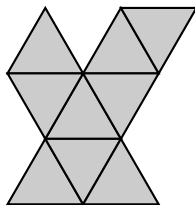


Figure 20: A polyform composed of 9 unit triangles

Polyominoes are polyforms made up of squares. Notice that for Definition 2.5, changing what polygons can be appended corresponds with changing the graph in which the connected subgraphs are constructed.

4.2 Generalization of Inscription

Minimal inscribed polyominoes can be extended to minimal inscribed polyforms. In the spirit of Definition 2.5, we consider the dual graph of the grid, representing the connection between cells.



Figure 21: A triangle in the triangular grid and its corresponding dual

In certain grids, it is clear what is considered a side. Figure 21 shows a triangle with 4 unit triangles touching each side of the larger triangle. However, it is less clear in other grids what is considered a side.

To designate what vertices belong to a side, label each vertex of the dual with a set containing the sides it belongs to. In general, we consider a dual graph G in which the nodes of each graph are labelled with subsets of $[k] = \{1, 2, \dots, k\}$, so that $\bigcup_{j \in V(G)} j = [k]$, where $V(G)$ is the vertex set of G . The variable k for this paper is informally the number of sides in the inscription shape. The grid for the minimal inscribed polyominoes is shown in Example 4.1.

Example 4.1. Inscription in the square grid is equivalent to inscription in the labelled dual below. We can call the family of $w \times \ell$ rectangles in the square grid $\square_{w,\ell}^S$, where S designates we are in a square grid.

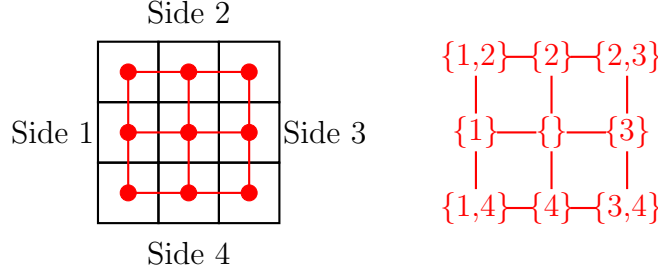


Figure 22: $\square_{3,3}^S$ and the labelled dual

This labelled dual, and all of $\square_{w,\ell}^S$, has $k = 4$ sides.

4.3 Minimal Inscribed Polyforms

Now we can define the polyomino equivalent in the labelled dual graph.

Definition 4.2. Suppose we have a labelled dual G . A given subgraph G' is an *inscribed polyform* in G if the following condition holds.

$$\bigcup_{j \in V(G')} j = [k] \quad (4)$$

Informally, condition 4 says that the subgraph G' touches all k sides. Notice that the number of vertices in an inscribed polyform of G can vary. If A is an inscribed polyform, then $|V(A)| \in [m(G), |V(G)|]$. Here $m(G)$ represents the minimum number of vertices for which Condition 4 holds, and can range from 1 to $|V(G)|$, depending on the structure and labelling of G .

Example 4.2. The labelled dual in Example 4.1 is $\square_{3,3}^S$, and so $m(R_{3,3}^S) = 5$. In general the family considered in Theorem 4, the $w \times \ell$ rectangular grid, has minimal area $m(R_{w,\ell}^S) = w + \ell - 1$.

Our focus is on the minimal inscribed polyforms, which are defined as follows.

Definition 4.3. An inscribed polyform A is *minimal* if $|V(A)| = m(G)$. Also let $\rho(G)$ denote the number of minimal inscribed polyforms in a given labelled graph G .

Our question is now how many *minimal inscribed polyforms* are there for a given labelled graph G ?

Example 4.3. Theorem 4 gives us that $\rho(R_{w,\ell}^S) = 8 \binom{w+\ell-2}{w-1} - 3w\ell + 2w + 2\ell - 8$.

4.4 New Results on Minimal Inscribed Polyforms

In this section we catalogue the known solved cases, which constitute the main new results of the paper. The methods used to solve the examples below are similar to that of Theorem 4. The total minimal inscribed polyforms are first split into certain subclasses that are easier to

count, analogous to S_2 , S_1 , and S_0 in Theorem 4). Each of these subclasses is then exactly enumerated, and combined to count the total.

Each result includes examples of each case for both the informal and dual graph definitions. Additionally, the labeling of the empty set will be replaced with a black node to simplify diagrams. The first solved case we will examine is the triangular analogue to Theorem 4.

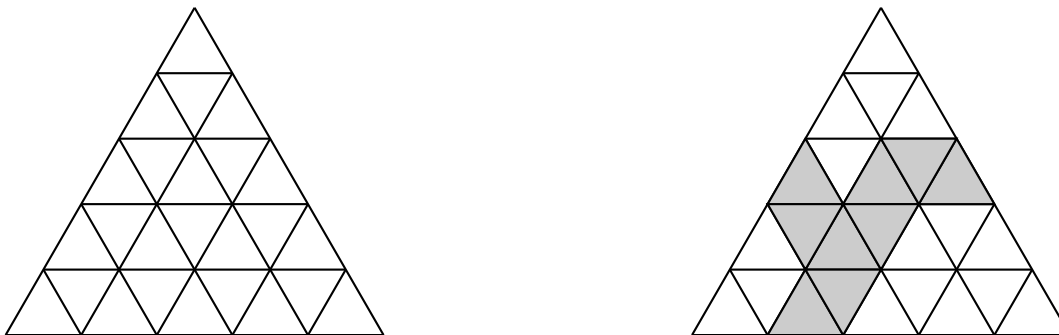


Figure 23: An $n = 5$ triangle in the triangular grid and a minimal inscribed polyform

Let us call the family of triangles one can make Δ_n^T , where n designates the number of triangles touching a side, and the superscript T designates that it is in a triangular grid.

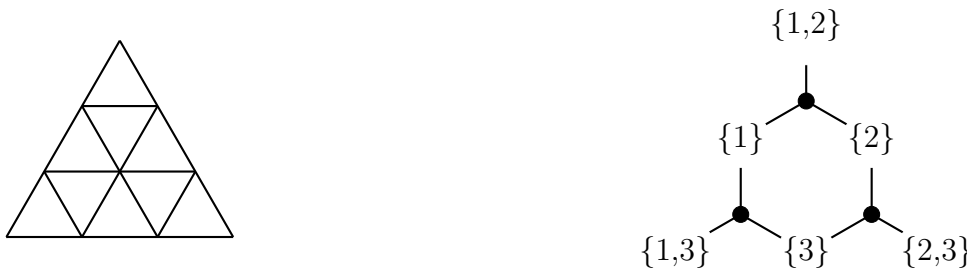


Figure 24: The $n = 3$ triangle in the triangular grid

Here $k = 3$, and $m(\Delta_n^T) = 2n - 1$.

Theorem 5. *The number of minimal inscribed polyforms $\rho(\Delta_n^T)$ for $n \geq 1$ is given by the following formula.*

$$\rho(\Delta_n^T) = ((n - 1)^2 + 2)2^{n-2}. \tag{5}$$

The first terms of this sequence, for $n \geq 1$, are 1, 3, 12, 44, 144, 432, 1216, . . .

The next solved family is similar.

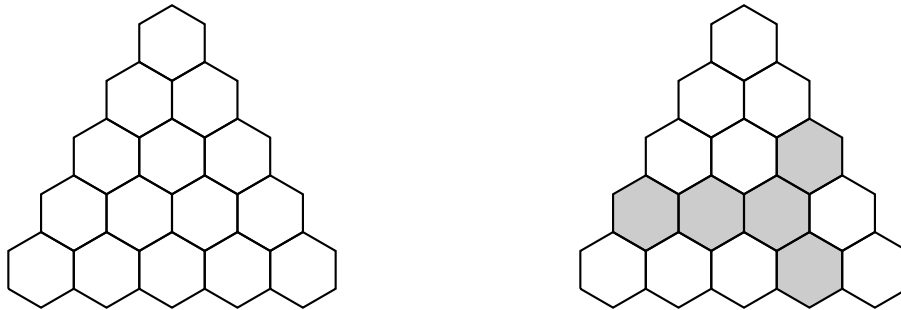


Figure 25: An $n = 5$ triangle in the hexagonal grid and a minimal inscribed polyform

Let us call the family of triangles you can make Δ_n^H , where n designates the number of hexagons touching a triangular side, and the superscript H designates that it is in a hexagonal grid.



Figure 26: The $n = 3$ triangle in the hexagonal grid

Here $k = 3$, and $m(\Delta_n^H) = n$.

Theorem 6. *The number of minimal inscribed polyforms $\rho(\Delta_n^H)$ for $n \geq 1$ is given by the following formula.*

$$\rho(\Delta_n^H) = \left(\binom{n}{2} + 2 \right) 2^{n-2}. \quad (6)$$

The first terms in this sequence, for $n \geq 1$, are 1, 3, 10, 32, 96, 272, 736, ... (A104270 [OEIS]).

The next solved family is below.

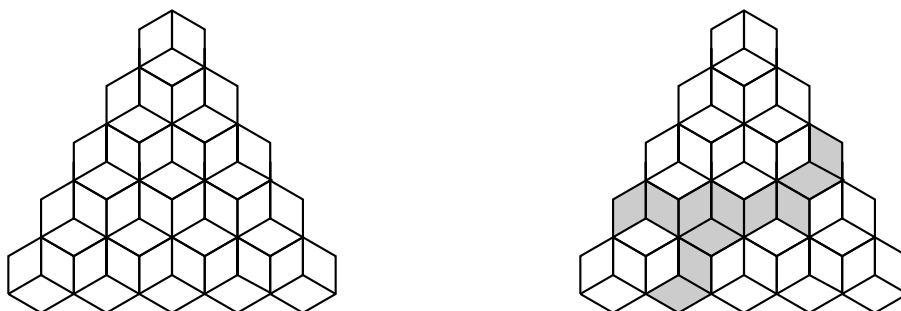


Figure 27: An $n = 5$ triangle in the rhombic grid and a minimal inscribed polyform

Let us call the family of triangles one can make Δ_n^R , where n designates the number of rhombuses touching a side, and the superscript R designates that it is in a rhombic grid.



Figure 28: The $n = 3$ triangle in the rhombic grid

Again $k = 3$, and $m(\Delta_n^R) = 2n + 1$.

Theorem 7. *The number of minimal inscribed polyforms $\rho(\Delta_n^R)$ for $n \geq 1$ is given by the following formula.*

$$\rho(\Delta_n^R) = n(n + 1)2^{n-2}. \tag{7}$$

The first terms of this sequence, for $n \geq 1$, are 1, 6, 24, 80, 240, 672, 1792, ... (A001788 [OEIS]).

The next solved family is below.



Figure 29: An $n = 5$ triangle in the bow tie grid and a minimal inscribed polyform

Let us call the family of triangles one can make Δ_n^B , where n designates the number of triangles touching a side, and the superscript B designates that it is a hexagonal and triangular grid, specifically the one above. This grid forms bow tie-like shapes with the triangles, and so earns the marking B for “bow tie grid.”



Figure 30: The $n = 3$ triangle in the bowtie grid

Again $k = 3$, and $m(\Delta_n^B) = 2n - 1$.

Theorem 8. *The number of minimal inscribed polyforms $\rho(\Delta_n^B)$ for $n \geq 2$ is given by the following formula.*

$$\rho(\Delta_n^B) = \left(n^2 + 3n + \frac{10}{3} \right) 4^{n-3} - \frac{1}{3} \quad (8)$$

The first terms of this sequence, for $n \geq 2$, starts 3, 21, 125, 693, 3669, 18733, ...

We can extend the dual in Figure 30. One can make $a - 2$ additional edge connections in a symmetric manner. This does not have an obvious analogue to grids, but interestingly can still be counted. We will call the family of these graphs $\Delta_n^{B,a}$, where B_a represents the grid-like dual with a connections, and n represents the size. $\Delta_2^{B,a}$ is shown below.

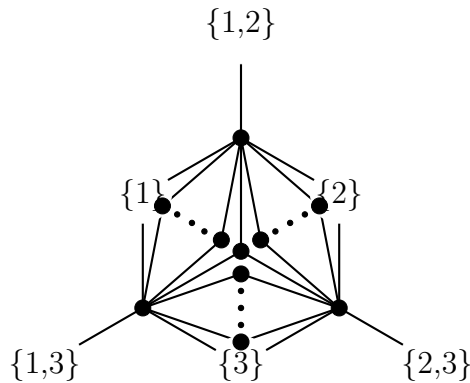


Figure 31: $\Delta_2^{B,a}$

Notice that we recover the bow tie grid for $a = 2$.

Theorem 9. *For a given $a \geq 2$, the number of minimal inscribed polyforms $\rho(\Delta_n^{B,a})$ for $n \geq 2$ is given by the following formula.*

$$\rho(\Delta_n^{B,a}) = U_a(n) a^{n-4} 2^{n-2} - 3(a^2 + 2a - 4) \left(\frac{a-2}{a-1} \right)^2 a^{n-4} + W_a(n), \quad (9)$$

where

$$U_a(n) = n^2 + \frac{(24a^3 - 44a^2 - 49a + 19)n}{(2a - 1)^2} + \frac{48a^5 - 216a^4 + 204a^3 + 258a^2 - 372a + 90}{(2a - 1)^3}$$

$$W_a(n) = 3 \left(\frac{2a - 3}{2a - 1} \right)^2 \left(\frac{a - 2}{a - 1} \right) n - \frac{48a^5 - 360a^4 + 1068a^3 - 1542a^2 + 1068a - 279}{(a - 1)^2(2a - 1)^3}.$$

The next solved family is below.



Figure 32: The 4×3 octagonal/square grid and a minimal inscribed polyform

Let us call the family of rectangles one can make $R_{w,\ell}^\theta$, where w designates how many octagons the grid is wide, and ℓ designates how many octagons the grid is long. R will indicate that we are forming a rectangle, and the superscript θ will indicate we are in the octagonal/square grid. Figure 32 is $R_{4,3}^\theta$.



Figure 33: The 3×3 rectangle in the octagonal/ square grid

Here $k = 4$, and $m(R_{w,\ell}^\theta) = w + \ell - 1$.

Theorem 10. *The number of minimal inscribed polyforms $\rho(R_{w,\ell}^\theta) = w + \ell - 1$ for $w, \ell \geq 1$ is given by the following formula,*

$$\rho(R_{w,\ell}^\theta) = 2D(w, \ell) - (w + 1)(\ell + 1) + 2 \sum_{i=0}^{w-1} \sum_{j=0}^{\ell-1} D(i, j)(2 + (w - 1 - i)(\ell - 1 - j)) \quad (10)$$

where $D(i, j)$ designates the i, j -th Delannoy number, which is given by

$$D(i, j) = \sum_{k=0}^{\min(i,j)} \binom{i+j-k}{i} \binom{i}{k}.$$

If we set $w = \ell = n$, we get a somewhat simplified formula.

$$\rho(R_{n,n}^\theta) = 2D(n, n) - (n + 1)^2 + 2 \sum_{i=0}^{n-1} \sum_{j=0}^{n-1} D(i, j)(2 + (n - 1 - i)(n - 1 - j)) \quad (11)$$

The first terms of this sequence, for $n \geq 1$, are 1, 6, 43, 256, 1401, 7510, . . .

It seems to be possible to enumerate many different types of families. One can even enumerate many families at once, as in $\Delta_n^{B,a}$. However, some simple families exhibit different behavior than these solved cases. These are the families that exhibit trivial growth.

4.5 Trivial Growth

The solved families we have seen so far have minimal inscribed polyforms growing exponentially in n . However, some families do not have a strictly increasing number of minimal inscribed polyforms in n at all. A family with this property have growth rate 1, and is referred to as a *trivial* family.

Example 4.4. An example of a labelled graph family that does not exhibit strictly increasing minimal inscribed polyforms is the family below.



Figure 34: The duals of $\square_{1,1}^{S^*}$ and $\square_{2,2}^{S^*}$

We will call this family $\square_{w,\ell}^{S^*}$ to match the new notation following Theorem 4. We only consider growth rates of the main diagonal, so we just look at $\square_{n,n}^{S^*}$.

Notice that for any $\square_{n,n}^{S^*}$, $n \geq 2$, the minimal path from the vertex labelled $\{1, 2\}$ to the vertex $\{3, 4\}$, and the minimal path from the vertex labelled $\{1, 4\}$ to the vertex labelled $\{2, 3\}$ will be the only 2 minimal inscribed polyforms. So for $n \geq 2$, $\rho(\square_{n,n}^{S^*}) = 2$.

There are other examples of trivial families. An interesting shape in combinatorics is the Aztec diamond. Let us call the family of Aztec diamonds A_n^S of width $2n$.



Figure 35: A_2^S and A_3^S

Their duals are

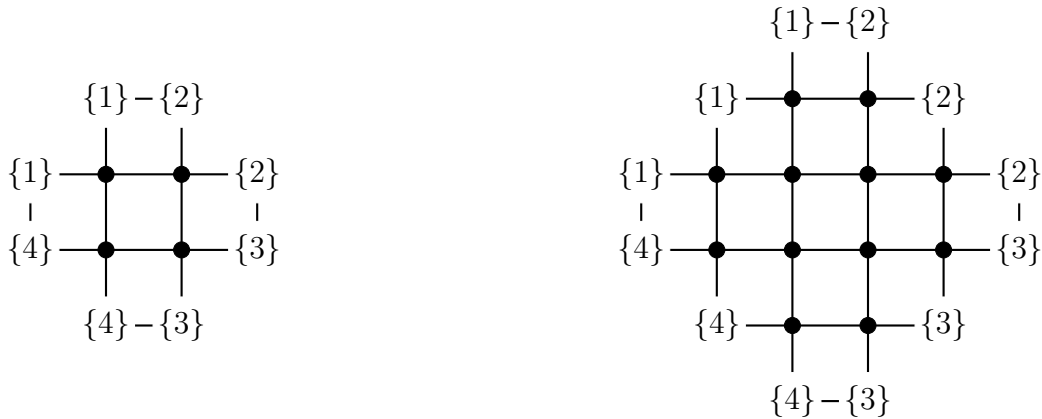


Figure 36: Duals of the $n = 2$ and $n = 3$ Aztec diamond

This family is trivial. Here, we have $k = 4$, and $m(A_n^S) = 2n + 2$. However, for $n \geq 2$, we have $\rho(A_n^S) = 4$, along with $\rho(A_1^S) = 1$. The 4 minimal inscribed polyforms that appear for $n \geq 2$ are shown in Figure 37.

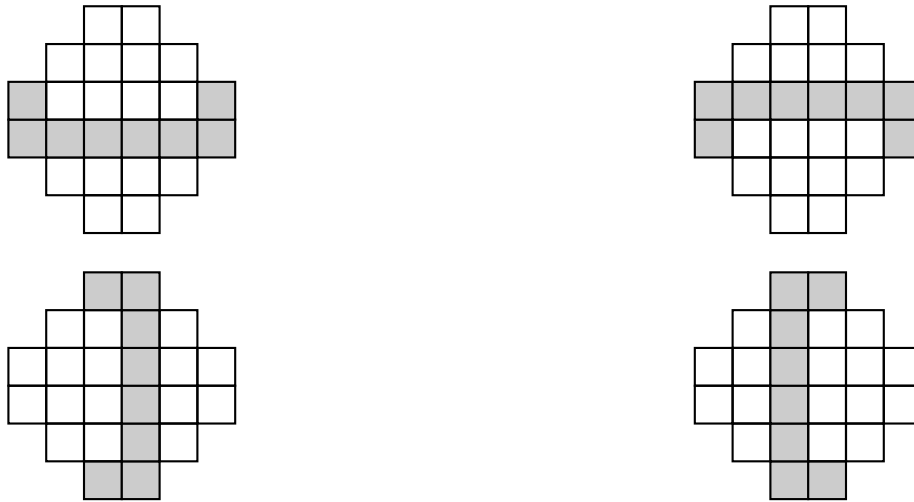


Figure 37: The 4 minimal inscribed polyforms in the $n = 3$ Aztec diamond

However, we can extend the duals for A_n^S . If we also consider cells diagonal from one another as adjacent, we can generate a new dual. Figure 39 represents family members of Aztec diamonds under this new dual.

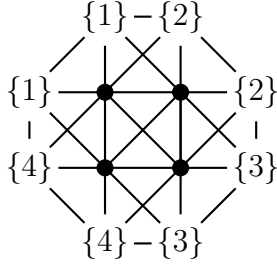


Figure 38: G_2

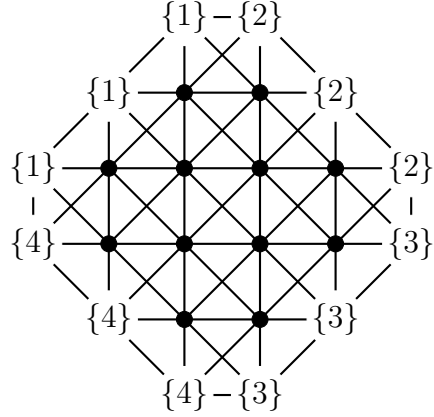
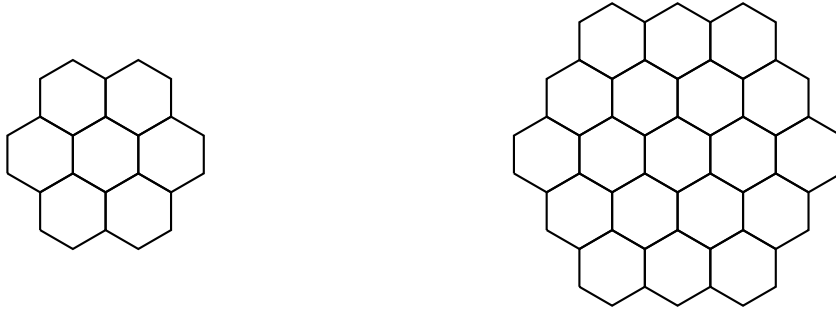


Figure 39: G_3

Figure 40: $A_1^{S^*}$ and $A_2^{S^*}$

We will call this family $A_n^{S^*}$. $A_n^{S^*}$ appears to be non-trivial. $\rho(A_n^{S^*})$ is known up to $n = 5$, where the first few terms are 1, 68, 1113, 11616, 104097. This appears exponential, but a conjectural exact formula for $\rho(A_n^{S^*})$ is unknown.

Interestingly, \square_n^S (a square inscribed in the square lattice) and \triangle_n^T (a triangle inscribed in the triangular lattice) both show non-trivial growth (Theorem 4 and Theorem 5), but the family \hexagon_n^H (a hexagon inscribed in the hexagonal grid) is trivial.



Above is \hexagon_2^H and \hexagon_3^H . The family \hexagon_n^H has $k = 6$, and $m(\hexagon_n^H) = 3n - 2$. For $n \geq 2$, we see a trivial ρ function, namely $\rho(\hexagon_n^H) = 2$. The subgraph shown in Figure 41 and its 60° degree rotation are the only 2 minimal inscribed polyforms.

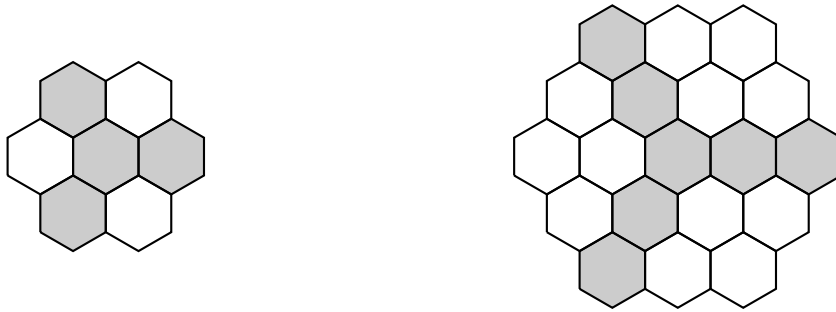


Figure 41: Minimal polyforms for grids in Figure 4.5

References

- [Ben74] Edward A. Bender. “Convex n -ominoes”. In: *Discret. Math.* 8 (1974), pp. 219–226.
- [BFR05] Elena Barucci, Andrea Frosini, and Simone Rinaldi. “On directed-convex polyominoes in a rectangle”. In: *Discrete Mathematics* 298.1 (2005). Formal Power Series and Algebraic Combinatorics 2002 (FPSAC’02), pp. 62–78. ISSN: 0012-365X. DOI: <https://doi.org/10.1016/j.disc.2005.01.006>. URL: <https://www.sciencedirect.com/science/article/pii/S0012365X05002335>.
- [BM04] Gill Barequet and Micha Moffie. “Counting Polyominoes on Twisted Cylinders”. In: *European Journal of Combinatorics* (Jan. 2004). DOI: 10.1145/2462356.2462357.
- [Dha82] Deepak Dhar. “Equivalence of the Two-Dimensional Directed-Site Animal Problem to Baxter’s Hard-Square Lattice-Gas Model”. In: *Phys. Rev. Lett.* 49 (14 Oct. 1982), pp. 959–962. DOI: 10.1103/PhysRevLett.49.959. URL: <https://link.aps.org/doi/10.1103/PhysRevLett.49.959>.
- [Gar65] Martin Gardner. “Mathematical Games: Pentominoes and Polyominoes”. In: *Scientific American* 213.4 (1965), pp. 96–105. ISSN: 00368733, 19467087. URL: <http://www.jstor.org/stable/24931159>.
- [GCN10] Alain Goupil, Hugo Cloutier, and Fathallah Nouboud. “Enumeration of Polyominoes Inscribed in a Rectangle”. In: *Discrete Appl. Math.* 158.18 (Nov. 2010), pp. 2014–2023. ISSN: 0166-218X. DOI: 10.1016/j.dam.2010.08.011. URL: <https://doi.org/10.1016/j.dam.2010.08.011>.
- [Ges99] Ira M. Gessel. “On The Number Of Convex Polyominoes”. In: *Unpublished Manuscript* (1999).
- [Gut09] Anthony Guttmann. “Polygons, Polyominoes and Polycubes”. In: *Lecture Notes in Physics* 775 (Jan. 2009). DOI: 10.1007/978-1-4020-9927-4.
- [Jen01] Iwan Jensen. “Enumerations of Lattice Animals and Trees”. In: *Journal of Statistical Physics* 102 (Feb. 2001), pp. 865–881. DOI: 10.1023/A:1004855020556.
- [Kla67] David A. Klarner. “Cell Growth Problems”. In: *Canadian Journal of Mathematics* 19 (1967), pp. 851–863. DOI: 10.4153/CJM-1967-080-4.
- [KR18] Matthew Kahle and Érika Roldán. *Polyominoes with maximally many holes*. 2018. DOI: 10.48550/ARXIV.1807.10231. URL: <https://doi.org/10.48550/arxiv.1807.10231>.
- [KR73] D. A. Klarner and R. L. Rivest. “A Procedure for Improving the Upper Bound for the Number of n -ominoes”. In: *Canadian Journal of Mathematics* 25.3 (1973), pp. 585–602. DOI: 10.4153/CJM-1973-060-4.
- [KR74] David A. Klarner and Ronald L. Rivest. “Asymptotic bounds for the number of convex n -ominoes”. In: *Discrete Mathematics* 8.1 (1974), pp. 31–40. ISSN: 0012-365X. DOI: [https://doi.org/10.1016/0012-365X\(74\)90107-1](https://doi.org/10.1016/0012-365X(74)90107-1). URL: <https://www.sciencedirect.com/science/article/pii/0012365X74901071>.

- [LC88] K. Y. Lin and S. J. Chang. “Rigorous results for the number of convex polygons on the square and honeycomb lattices”. In: *Journal of Physics A: Mathematical and General* 21.11 (June 1988), pp. 2635–2642. DOI: 10.1088/0305-4470/21/11/020. URL: <https://doi.org/10.1088/0305-4470/21/11/020>.
- [Mad99] Neal Madras. “A pattern theorem for lattice clusters”. In: *Annals of Combinatorics* 3 (1999), pp. 357–384.
- [OEIS] Neil J. A. Sloane and The OEIS Foundation Inc. *The Online Encyclopedia of integer sequences*. URL: <http://oeis.org/?language=english>.
- [PS81] Giorgio Parisi and Nicolas Sourlas. “Critical Behavior of Branched Polymers and the Lee–Yang Edge Singularity”. In: *Phys. Rev. Lett.* 46 (14 Apr. 1981), pp. 871–874. DOI: 10.1103/PhysRevLett.46.871. URL: <https://link.aps.org/doi/10.1103/PhysRevLett.46.871>.
- [Tem56] H. N. V. Temperley. “Combinatorial Problems Suggested by the Statistical Mechanics of Domains and of Rubber-Like Molecules”. In: *Phys. Rev.* 103 (1 July 1956), pp. 1–16. DOI: 10.1103/PhysRev.103.1. URL: <https://link.aps.org/doi/10.1103/PhysRev.103.1>.